Critical Reviews in Biochemistry and Molecular Biology

ISSN: 1040-9238 (Print) 1549-7798 (Online) Journal homepage: http://www.tandfonline.com/loi/ibmg20

MarR family transcription factors: dynamic variations on a common scaffold

Dinesh K. Deochand & Anne Grove

To cite this article: Dinesh K. Deochand & Anne Grove (2017) MarR family transcription factors: dynamic variations on a common scaffold, Critical Reviews in Biochemistry and Molecular Biology, 52:6, 595-613, DOI: 10.1080/10409238.2017.1344612

To link to this article: http://dx.doi.org/10.1080/10409238.2017.1344612

CRITICAL REVIEWS IN BIOCHEMISTRY AND MOLECULAR BIOLOGY, 2017
VOL. 52, NO. 6, 595–613
https://doi.org/10.1080/10409238.2017.1344612

Taylor & Francis
Taylor & Francis Group

REVIEW ARTICLE

MarR family transcription factors: dynamic variations on a common scaffold

Dinesh K. Deochand* and Anne Grove

Department of Biological Sciences, Louisiana State University, Baton Rouge, LA, USA

ABSTRACT

Members of the multiple antibiotic resistance regulator (MarR) family of transcription factors are critical for bacterial cells to respond to chemical signals and to convert such signals into changes in gene activity. Obligate dimers belonging to the winged helix-turn-helix protein family, they are critical for regulation of a variety of functions, including degradation of organic compounds and control of virulence gene expression. The conventional regulatory paradigm is based on a genomic locus in which the gene encoding the MarR protein is divergently oriented from a gene under its control; MarR binding to the intergenic region controls expression of both genes by changing the interaction of RNA polymerase with gene promoters. MarR protein oxidation or binding of a small molecule ligand adversely affects DNA binding, resulting in altered expression of the divergent genes. The generality of this simple paradigm, including the regulation of *Escherichia coli* MarR by direct binding of antibiotics, has been challenged by reports published in recent years. In addition, structural and biochemical analyses of ligand binding to numerous MarR homologs are converging to identify a shared ligand-binding "hot-spot". This review highlights recent research advances that point to shared features, yet at the same time highlights the remarkable flexibility with which members of this protein family implement responses to inducing signals. A more comprehensive understanding of protein function will pave the way towards the development of both antibacterial agents and biosensors that are based on MarR family proteins.

ARTICLE HISTORY
Received 2 May 2017
Revised 15 June 2017
Accepted 16 June 2017

KEYWORDS
Gene regulation; ligand-binding; MarR; protein–DNA interaction; protein oxidation; transcription factor

Introduction

Bacteria respond to environmental agents or a change in intracellular metabolites by modulating gene regulatory networks. For example, pathogens may oscillate between saprophytic or pathogenic phases and must adapt to the hostile environment created by host defenses (Groisman and Mouslim 2006). Such changes in gene expression may be mediated by transcription factors, which bind to specific sites and tweak the activity of cognate genes. MarR (multiple antibiotic resistance regulator) family transcriptional regulators feature predominantly in this context as their activity modulates numerous cellular processes, including stress responses, virulence, and degradation of harmful chemicals. The *marR* gene was first characterized in *Escherichia coli* and reported to encode a transcription factor that regulates the multiple antibiotic resistance (*marRAB*) operon, which confers resistance to antibiotics, phenolic compounds, organic solvents, and household disinfectants (Alekshun and Levy 1999b, 2007).

The MarR protein family is thought to have originated before the divergence of bacteria and archaea, and the proteins are ubiquitous in these species. Ensembl Bacteria hosts the annotation of more than 44,000 bacterial and archaeal genomes (Kersey *et al.* 2016). A search of this database for "MarR" returns almost 335,000 hits, suggesting about seven MarR proteins per genome. The distribution is uneven, however, with obligate parasitic species with reduced genome sizes encoding few transcription factors (including MarRs) and species characterized by large genomes and a complex lifestyle encoding many (Perez-Rueda *et al.* 2004). For example, a search of Ensembl Bacteria returns no MarR homologs in *Helicobacter pylori* 26695, a specialized gastric pathogen, but 35 paralogs in the soil saprophyte *Streptomyces coelicolor* A3(2), which is characterized by a complex secondary metabolism. Often, genes encoding MarR proteins are divergent from a gene or operon under their control and MarR proteins may either repress or activate expression of genes in their regulons (Figure 1). DNA binding by MarR proteins is altered in the presence of specific signals or ligands, resulting in differential gene expression (Perera and Grove 2010a).

CONTACT Anne Grove agrove@lsu.edu Department of Biological Sciences, Louisiana State University, Baton Rouge, LA 70803, USA
*Current address: Hospital for Special Surgery, New York, NY, USA.

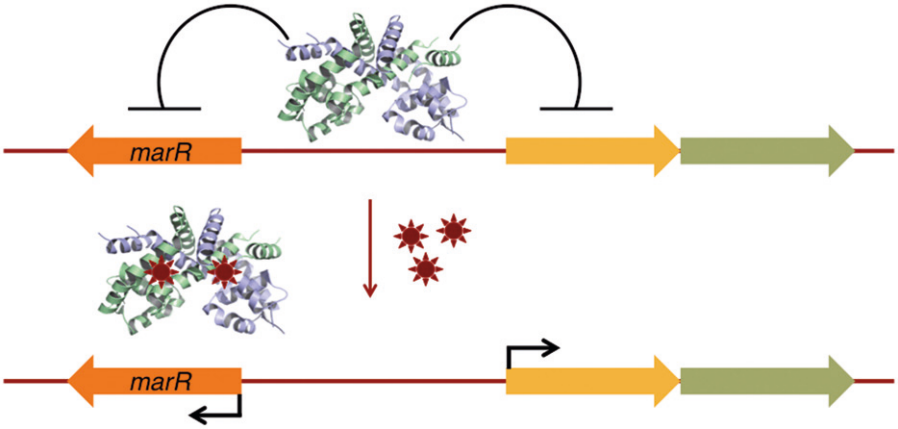

Figure 1. A typical organization of genetic loci encoding MarR proteins. MarR regulates the activity of *marR* and a divergently oriented gene or operon by binding to the intergenic region. DNA binding of MarR is modulated in presence of specific chemical signals, resulting in differential gene expression. (see color version of this figure at www.tandfonline.com/ibmg).

Structures of MarR homologs show that the proteins exist as dimers with each subunit contributing a winged helix-turn-helix (wHTH) DNA-binding motif (Alekshun *et al.* 2001, Hong *et al.* 2005, Bordelon *et al.* 2006, Perera and Grove 2010a). The DNA binding lobes are spatially configured such that recognition helices can interact with consecutive DNA major grooves. The majority of MarR family proteins bind recognizable palindromic sequences within the intergenic region of divergently oriented genes, resulting in attenuation of gene expression by sterically hindering the binding of RNA polymerase to the promoter. While direct obstruction of RNA polymerase binding to the promoter is a common consequence of MarR protein binding to gene promoters, alternate modes of derepression exist, including prevention of open complex formation, interference with promoter escape and elongation by RNA polymerase, as well as a novel mode of regulation in which the MarR protein induces changes in promoter DNA topology in the repressive mode, whereas such changes in DNA conformation are attenuated in the permissive binding mode (Galan *et al.* 2003, Deochand *et al.* 2016a). In addition, some MarR homologs function as activators either by binding to the upstream region of the promoter and stabilizing RNA polymerase or by competing for promoter binding by a repressor (Tran *et al.* 2005, Curran *et al.* 2017).

The emerging picture of MarR-dependent gene regulation reflects a conserved structural framework and the existence of a shared ligand-binding pocket that when occupied affects either structure or dynamics of the dimer interface or the DNA-binding lobes. However, it is becoming evident that protein flexibility and dynamics vary between MarR homologs, leading to different mechanisms by which protein binding to DNA affects the ability of RNA polymerase to bind and initiate transcription and to distinct responses to inducing signal. A complete mechanistic understanding of MarR protein function in turn opens prospects for utilizing such proteins in synthetic biosensor devices in which biochemical reactions are initiated as a consequence of the transcription factor responding to cognate chemical signals.

Dynamics of dimer interface and DNA recognition helices

Structural framework of MarR proteins

Structural information for multiple MarR homologs shows that they exist as homodimers (Alekshun *et al.* 2001, Bordelon *et al.* 2006). The only possible exception is *Thermoplasma volcanium* MLPTv, a structural homolog of MarR with unknown biological function that was reported to exist as a monomer (Liu *et al.* 2010). These authors also reported that MLPTv has an evenly hydrated surface, consistent with its existence as a monomer.

Each MarR subunit is usually composed of six α-helices and three β-strands with α1–α2–β1–α3–α4–β2–β3–α5–α6 topology (Figure 2(A)). Overall, the dimer adopts a pyramidal shape with pseudo-2-fold symmetry (Figure 2(B)). A subset of MarR homologs that was designated as the UrtR (urate-responsive transcriptional regulator) protein family based on the founding member *Deinococcus radiodurans* HucR differs by including an *N*-terminal extension (Perera and Grove 2011). The structure of HucR shows that this extension forms an α-helix that braces the *N*-terminus of α1, which connects the dimerization and DNA binding regions (Bordelon *et al.* 2006).

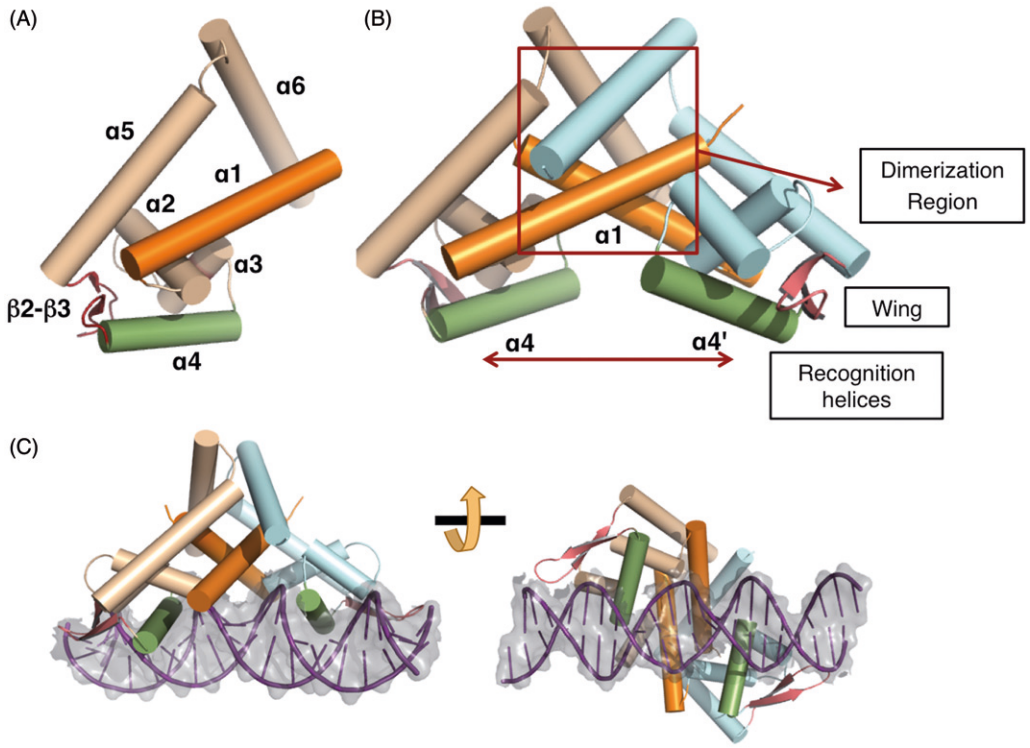

Figure 2. Structural features of MarR proteins. (A) MarR subunit with secondary structure elements identified. Secondary structure element β1 connects helices α2 and α3 and is hidden from view. (B) The two long intersecting helices (α1; gold) form the scaffold for the dimerization domain. Recognition helices (α4; green) contact DNA in consecutive major grooves, and wings (red) bind adjacent minor grooves. Based on PDB ID: 3QPT (*S. enterica* SlyA). (C) MarR protein in complex with double stranded DNA. The recognition helices (α4; green) interact with consecutive major groove whereas the wing (red) contacts adjacent minor grooves. Based on PDB ID: 3Q5F (*S. enterica* SlyA with operator DNA). Figure generated with PyMol. (see color version of this figure at www.tandfonline.com/ibmg).

Analysis of crystal structures of MarR proteins reveals that each subunit contributes a dimerization region and a DNA binding lobe. The dimerization region is formed by an interdigitation of *N*- and *C*-terminal helices α1, α5, and α6 from both subunits that buries significant surface area, with the interaction between the two long antiparallel helices from each subunit (α1/α1′) forming the scaffold and helices α5 and α6 straddling α1′ and α5′/α6′ straddling α1 (where prime denotes the other subunit; Figure 2(B)) (Alekshun *et al.* 2001, Bordelon *et al.* 2006). The internal faces of these helices that join to form the dimer interface are hydrophobic, a feature that is conserved among MarR proteins (Kumaraswami *et al.* 2009). Confirming the importance of these interactions, deletion of the *C*-terminal 18 amino acids of *E. coli* MarR reduces the ability to form dimers, which in turn results in attenuated DNA binding and an antibiotic resistance phenotype *in vivo* (Alekshun *et al.* 2000). Similarly, terminal deletions of *Yersinia pseudotuberculosis* RovA result in compromised dimerization or inability to express the mutant proteins (Tran *et al.* 2005). The dynamics of the dimer interface can also modulate DNA binding by altering the distance between DNA recognition helices, and changes in the dimer interface can affect fidelity or strength of the protein–DNA interaction (Andresen *et al.* 2010, Deochand *et al.* 2016b). Such communication between the dimerization region and the DNA-binding motif is in large part due to the long *N*-terminal scaffold helices α1/α1′, whose *C*-termini interact with the HTH motifs, as well as α5/α5′, which follow the wing motifs and whose *C*-terminal halves straddle the *N*-termini of α1′/α1. Specifically, it has been shown that flexibility of the dimer interface may be required for MarR proteins to adopt a conformation compatible with binding consecutive DNA major grooves, as discussed below.

The DNA binding motif is composed of β1–α3–α4–β2–β3, which adopts the winged-helix fold. The "wing" is composed of the two antiparallel beta strands β2 and β3 and it is highly flexible and thus not well resolved in most crystal structures in absence of DNA (Alekshun *et al.* 2001, Lim *et al.* 2002, Bordelon *et al.* 2006, Dolan *et al.* 2011). The winged-helix motif is a variant of the HTH and it is a signature of MarR homologs. The wHTH part invariably binds the DNA major groove by insertion of the second helix of the

motif, the recognition helix (α4) (Hong *et al.* 2005, Dolan *et al.* 2011). The DNA-binding lobes of each subunit generally function independently, and they are locally stabilized by hydrophobic interactions, forming a compact fold. The electrostatic surface potential characteristic of the DNA-binding region is strongly electropositive, which is beneficial for interacting with DNA. Although MarR homologs adopt similar topological configurations, the structural plasticity affords them the ability to bind disparate DNA targets. Structural analyses also indicate that some MarR proteins appear capable of adopting a conformation that is compatible with DNA binding in their unliganded form, while others do not and would have to undergo conformational changes to be able to engage cognate DNA.

DNA binding dynamics

Binding to adjacent DNA major grooves on the same face of the DNA duplex

MarR family transcription factors bind cognate DNA as a dimer, associating with 16–20 bp (pseudo) palindromic double-stranded DNA (Hong *et al.* 2005, Kumarevel *et al.* 2009, Perera and Grove 2010a, Dolan *et al.* 2011). The only exception is *Staphylococcus epidermidis* TcaR, which was shown to interact strongly and cooperatively with single-stranded DNA (ssDNA) (Chang *et al.* 2014). Structural data of multiple MarR proteins in complex with DNA show that the recognition helices (α4) of the DNA binding lobes contact two consecutive major grooves whereas the wing of the wHTH motif interacts with adjacent minor grooves (Figure 2(C)).

Mutation of amino acids in both the recognition helix and the wing verify roles in DNA binding. For *E. coli* MarR, replacement of Arg73 with Cys in the recognition helix abolishes DNA binding in whole cells as well as *in vitro*. Also, the mutation of Arg94 to Cys at the tip of the wing inactivates the repression function of MarR in a whole cell assay, whereas a replacement of Gly95 with Ser in the same region increases the DNA binding affinity by 30-fold (Alekshun and Levy 1999a). In HucR, mutation of Arg118 in the wing also compromises binding; in general, this Arg (which is conserved in MarRs) is thought to contribute to affinity, not specificity (Wilkinson and Grove 2005).

Although MarR proteins share the structural element that contacts promoter DNA, affinity and mode of DNA binding differs. MarR proteins may associate with their cognate DNA as a single dimer or as multimers, sometimes stabilized by protein–protein interaction. For instance, *D. radiodurans* HucR binds as a single dimer to its operator region to repress divergent genes encoding HucR and the enzyme uricase (Wilkinson and Grove 2004). DNase I footprinting of *Pseudomonas aeruginosa* MexR, which controls expression of an antibiotic efflux pump, suggests binding of two dimers to two independent palindromic sites of 28 bp separated by 3 bp (Lim *et al.* 2002). Footprinting of *Dickeya dadantii* MfbR reveals that it protects a single site of 48 bp, however, at higher protein concentrations the protection increases to 60 bp, suggesting that the extended protection might be due to protein-protein interaction (Reverchon *et al.* 2010). Likewise, *S. coelicolor* TamR, which controls expression of genes associated with the citric acid cycle, first binds a preferred palindromic site in the *tam–tamR* intergenic DNA with very high affinity (K_d ~16 pM), followed by accretion of protein to associate with five overlapping sites, with adjacent TamR dimers predicted to reside on opposite faces of the DNA duplex (Huang and Grove 2013).

In some instances, individual MarR proteins have been reported to bind different operator sites with distinct stoichiometries. For example, while TamR binds six overlapping sites in *tam–tamR* intergenic DNA, it binds two overlapping sites in the *aceB1* promoter driving expression of malate synthase and a single palindromic site upstream of genes encoding malate dehydrogenase and isocitrate synthase (Huang *et al.* 2013, 2015). *Agrobacterium fabrum* PecS binds a single palindromic sequence in the *pecS* promoter, but more stably to two overlapping sites that span the divergent *pecM* promoter and coding region (Perera and Grove 2010b), and *Staphylococcus aureus* MepR similarly binds the *mepR* promoter as a single dimer, but as a dimer-of-dimers and with greater affinity to two inverted repeats in the adjacent *mepA* promoter. As a consequence, repression of *mepA* is complete, whereas *mepR* expression is leaky (Kaatz *et al.* 2006, Kumaraswami *et al.* 2009). Thus, such differences in stoichiometry of binding may contribute to differential gene expression.

While most MarR proteins are sequence specific, many have been reported to interact with degenerate sequences. For example, crystallization of *S. aureus* MepR, which controls expression of a multidrug efflux pump, revealed specific MepR-DNA complexes plus an additional dimer bound to DNA in a different configuration, proposed to reflect nonspecific binding; almost all contacts are to the DNA backbone albeit with fewer contacts than observed for specific MepR–DNA complexes and the wing contacts different bases in the minor groove (Birukou *et al.* 2014). Consistent with the ability of some MarR proteins to interact with degenerate sequences, alignment of promoters controlling expression of genes in the *D. dadantii* PecS regulon reveals little sequence conservation (Praillet *et al.* 1996, Rouanet *et al.* 1999).

Footprinting of *E. coli* MarR suggests that it binds two sites (~21 bp each) in *marO* DNA. Each MarR binding site was proposed to be composed of 5 bp inverted repeats separated by 2 bp, which would position each half-site on opposite faces of the double helix DNA (Alekshun *et al.* 2000, 2001). However, the recently published structure of *E. coli* MarR in complex with cognate DNA revealed the expected interaction of recognition helices in consecutive major grooves on the same face of the duplex, albeit with a modest global bend of almost 9° and a widening of DNA major grooves upon protein binding; this structure was achieved using a Cys80Ser mutant in which oxidation to yield a conformation incompatible with DNA is prevented (Zhu *et al.* 2017). A better description of cognate sites for *E. coli* MarR is therefore 8 bp imperfect repeats, which would place each half-site on the same face of DNA. By comparison to the structure of apo-MarR, DNA binding imposes an ~27° rotation of wHTH motifs to widen the distance between recognition helices to ~29 Å and allow interaction in consecutive DNA major grooves. Similarly, MexR protects two regions of ~28 bp and each site is composed of 5 bp half-sites separated by 5 bp such that the centers of each half-site are on the same face of the DNA. The recognition helices in the open conformation of MexR are separated by 29.2 Å, compared to the 34 Å distance between the centers of each half-site in linear *B*-form DNA, which suggests that conformational change in either protein and/or DNA occur upon DNA binding (Lim *et al.* 2002).

Conformational changes in both DNA and protein

Conformational changes in MarR proteins required for DNA binding or a distortion of DNA induced upon complex formation is evident from several crystal structures of MarR proteins in complex with cognate DNA. *Bacillus subtilis* OhrR was co-crystallized with 29 bp *ohrA* operator DNA that encompasses the −10 promoter element and the protein was shown to bind as a single dimer (Hong *et al.* 2005). Although OhrR binds *B*-form DNA, it imposes DNA bending by 10° and causes undertwisting resulting in shortening of the binding site by 3.5 Å. Moreover, interaction with recognition helices causes widening of the major grooves by 5.5 Å. Each recognition helix has few contacts with DNA major grooves, however, the *N*-termini are pointed towards the floor of the major grooves to make base-specific contacts. Further, the complex is stabilized by the wing region of the wHTH motif. The wing of OhrR is longer in comparison to other prokaryotic wHTH motifs; it spans over 67 Å with tip insertion in the minor groove, inducing local overtwisting by ~7°. Both recognition helices and wings contact DNA directly and interactions are maintained by water-mediated hydrogen bonds, van der Waals contacts, or electrostatic interactions. Besides the main binding elements, OhrR contains a third DNA binding element, a helix–helix motif (HH) composed of α1 and α2, that buttresses the DNA binding by contacting the phosphate backbone.

Salmonella enterica SlyA also induces conformational changes in its 22 bp cognate DNA (Dolan *et al.* 2011). The SlyA-bound DNA is globally bent towards the bottom of the SlyA dimer, imposing a kink of ~16° as well as local undertwisting of DNA by 1.2° at the middle of the pseudo-palindromic site. SlyA makes similar contacts with DNA as OhrR, but Arg 86 in the wing of SlyA plays a key role in interacting with the DNA minor groove. It has been reported that SlyA makes a large number of contacts with the DNA backbone in comparison to base-specific interaction and it has been proposed that binding of SlyA relies upon the shape of the DNA rather than specific sequence for binding. Thus, this mechanism enables SlyA to mediate global regulatory function by binding to degenerate sequences; indeed, the consensus sequence for *S. enterica* serovar Typhimurium was limited to three base pairs per half-site ($TTAN_6TAA$) and a similar consensus was suggested for *E. coli* SlyA (Haider *et al.* 2008, Curran *et al.* 2017).

S. aureus MepR, crystallized in the presence of the 27 bp *mepR* site, binds DNA similarly to other MarR proteins, however, it utilizes a unique mechanism to recognize specific sites based solely on van der Waals interactions (Birukou *et al.* 2014). The *N*-termini of the recognition helices insert into major grooves similarly to other MarR proteins, however, they contact bases only by van der Waals interactions. Although the wHTH motif from each subunit contact major grooves and the wing is inserted into the flanking AT-rich minor grooves, the majority of protein–DNA interactions are nonspecific. The amino acid residues of the wHTH motif contact the sugar–phosphate backbone of DNA by hydrogen bonds or salt bridges. By contrast, the structure of ST1710, a *Sulfolobus tokodaii* MarR homolog in complex with DNA reveals a distinct organization, in which only the wing motif contacts DNA specifically *via* bases in the minor grooves (Kumarevel *et al.* 2009). The DNA recognition helices make neither specific or direct contact with DNA bases, nor insert into the major grooves. Additionally, large unequal conformational changes were observed in both subunits of ST1710. One of the subunits was displaced by 13 Å to reorient itself on the DNA binding site. The DNA binding motif is elevated in one subunit whereas helix α6 is lower in the other. Notably, the distance between wHTH domains in the dimer is increased

by 10 Å for the protein–DNA complex in comparison to unbound protein.

Rigid body movements of wHTH motifs required for DNA binding have also been reported, as exemplified for *E. coli* MarR (Zhu *et al.* 2017). The co-crystal structure was reported for MarR-Cys80Ser, a mutant that retains DNA binding, but is insensitive to oxidation. A comparison with apo-MarR-Cys80Ser shows that the reorientation of the wHTH motifs is a consequence of conformational changes in α5, which connects the wHTH and dimerization regions. DNA binding is linked to a disruption of α5 by formation of an internal loop centered at Gly116; the flexibility imposed by Gly116 is critical for DNA binding as evidenced by attenuated DNA binding when this residue is mutated (Zhu *et al.* 2017). Curiously, the breakage of α5 that is required for DNA binding by *E. coli* MarR was previously seen in other MarRs, including *Xanthomonas campestris* OhrR, except that disruption of α5 in this case was associated with protein oxidation to attain a conformation in which the protein cannot bind DNA (Newberry *et al.* 2007). These conformational changes indicate that structural flexibility of MarR proteins is required for optimal DNA binding.

Binding of ssDNA by TcaR

While most studies have reported that MarR homologs interact with dsDNA, it has been recently found that *S. epidermidis* TcaR, which is linked to control of biofilm formation, strongly binds single-stranded DNA in addition to dsDNA (Chang *et al.* 2014), suggesting a novel regulatory mechanism. Major structural changes were observed in the wHTH region when TcaR binds ssDNA. The wHTH motif of both subunits twist with respect to each other, resulting in a sheared orientation that causes shortening of the distance between the *C*-termini of helices α3/α3′ by 11.8 Å compared to TcaR–dsDNA complex model. Moreover, the binding of ssDNA to TcaR displaces the wing by 18 Å from its likely position in the dsDNA minor groove. This motion generates an asymmetrical conformation, which is unfavorable for interaction with dsDNA. Therefore, different modes of interaction are proposed in the ssDNA–TcaR and dsDNA–TcaR complexes, even though the binding sites are similar. These findings suggest that TcaR protein might play a role in resistance against ssDNA phage infection in bacterial pathogens.

Taken together, structural details of MarR proteins in complex with DNA combined with biochemical studies reveal a remarkable ability of MarR proteins to recognize different DNA targets and showcase their multi-dimensional mode of binding and the distinct structural rearrangements needed for DNA binding.

Allosteric modulation of DNA binding

DNA binding by MarR proteins is modulated by chemical signals, either ligands such as small phenolic molecules or metals or reactive oxygen species that modify reactive cysteines (Perera and Grove 2010a, Grove 2013). Considering the importance of MarR proteins in antibiotic resistance as well as other cellular functions, many studies have focused on identification of effector molecules and the mechanism by which they control MarR protein function. While identification of cognate DNA sequences generally poses less of a challenge, considering the frequent occurrence of palindromic sequences in *marR* gene promoters, identification of effector signals has proven more difficult.

E. coli MarR

Early efforts at understanding mechanisms of ligand-mediated attenuation of DNA binding by MarR family members were principally based on *E. coli* MarR, co-crystallized in presence of salicylate (Alekshun *et al.* 2001). Salicylate abrogates MarR activity both *in vitro* and *in vivo* at millimolar concentrations, resulting in activation of MarA, thereby inducing multiple antibiotic resistance phenotypes. The crystal structure of MarR bound to salicylate revealed two SAL binding sites per subunit, both of which highly solvent exposed and on either side of the proposed DNA binding helix α4. Later, the physiological relevance of these salicylate-binding sites was brought into question, since very high concentration of salicylate (~250 mM) was used to grow the crystals. Subsequently, Duval *et al.* (2013) showed that mutations in the original SAL sites had no effect on salicylate binding, which corroborated the concern that the originally identified sites were artifacts of using excess salicylate (Duval *et al.* 2013).

More recently, *in vivo* studies suggested that salicylate instead induces envelope stress and release of copper, leading to copper-mediated oxidation of MarR and induction of a multiple antibiotic resistance phenotype (Hao *et al.* 2014). The modification of MarR is specific to Cu(II), with no effect on DNA binding seen *in vitro* on addition of either H_2O_2 or other divalent transition metals to MarR. Cu(II) directly and reversibly oxidizes Cys80 in *E. coli* MarR and triggers the formation of a disulfide bond between two MarR dimers (Hao *et al.* 2014) (Figure 3). Upon formation of a tetrameric complex, the DNA recognition helices get sequestered within the interface between two MarR dimers, precluding DNA

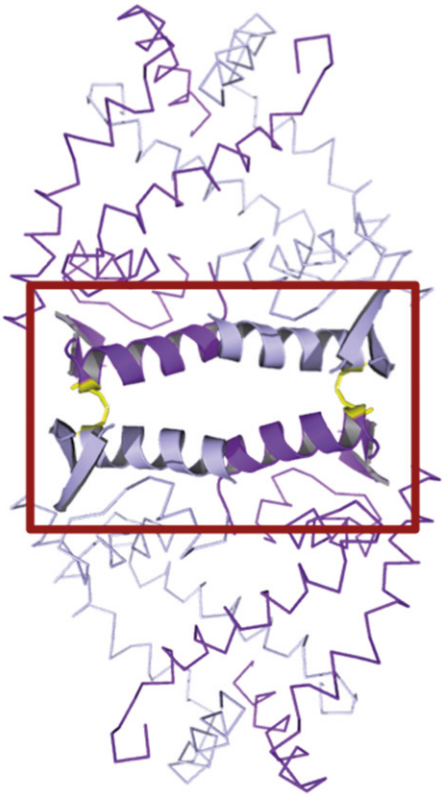

Figure 3. Oxidized *E. coli* MarR. Cu^{2+} oxidizes Cys80 in recognition helices (cartoon representation) to generate disulfide bonds (yellow) between two MarR dimers (represented as ribbon with each subunit in blue and purple). Recognition helices are buried in the tetramer, precluding DNA binding. Based on PDB ID: 4JBA. Figure generated with PyMol. (see color version of this figure at www.tandfonline.com/ibmg).

binding. The Cu(II) may be released from the bacterial envelope due to oxidative damage of membrane proteins *via* envelope stress imposed by exposure to antibiotics such as salicylate, ampicillin, and norfloxacin (Hao *et al.* 2014).

A "hot spot" for antagonist binding

Salicylate as a ligand

Several additional MarR proteins have been co-crystallized with salicylate, including *S. tokodaii* ST1710 (Kumarevel *et al.* 2009), *Methanobacterium thermoautotrophicum* MTH313 (Saridakis *et al.* 2008), *S. epidermidis* TcaR (Chang *et al.* 2010), and *S. enterica* SlyA (3DEU; unpublished). Analysis of ligand-free and salicylate-bound structures of ST1710 and MTH313 revealed that two salicylate molecules bind to one dimer. One molecule binds in a deep binding pocket located at the junction of dimerization and DNA-binding regions (SAL1) whereas the other ligand-binding site (SAL2) is positioned 5 Å away from the symmetrical site (Figure 4). Only binding of salicylate at site SAL1 induces a large conformational change in MTH313 in comparison to apo-protein, apparently sufficient to preclude DNA binding (Saridakis *et al.* 2008). This suggests that SAL1 is the biologically relevant site. Conversely, no structural rearrangements were found between apo and ligand-bound ST1710, suggesting that either salicylate is not a true ligand for ST1710 or it stabilizes a closed conformation of the protein that is incapable of interacting with DNA.

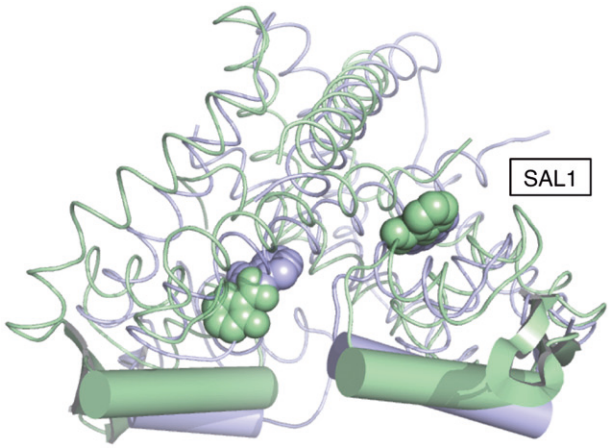

Figure 4. Ligand binding pocket shared among many MarR proteins. The figure is generated from all-atom superposition of *S. epidermidis* TcaR-salicylate (light blue; PDB ID: 3KP6) and *M. thermoautotrophicum* MTH313-salicylate (green; PDB ID: 3BPX). In MTH313, occupancy of the salicylate binding pocket at the right (SAL1) is associated with conformational changes and is considered physiologically relevant. Salicylate is shown in space-filling representation and recognition helices in cartoon. Note that salicylate occupies the same position in the SAL1 binding pocket in both structures. Figure generated with PyMol. (see color version of this figure at www.tandfonline.com/ibmg).

In contrast, eight molecules of salicylate bound to one TcaR dimer. Each binding sites was distinct and designated as SAL1 to SAL8. Of these sites, two salicylate molecules were present in similar binding pockets as described in MTH313, while two bound in more shallow binding pockets in each monomer. The remaining ligands were highly exposed to the solvent. In addition to salicylate, TcaR was also crystallized in complex with four antibiotics (ampicillin, kanamycin, methicillin, and penicillin G) (Chang *et al.* 2010). Unlike salicylate, all antibiotics bound TcaR at only two sites per dimer; one compound was located in the cavity at the intersection of the dimerization region and the DNA-binding motif and the other was near the DNA recognition helices α4 at the interface of three TcaR dimers. Superposition of native and salicylate/antibiotic-bound TcaR complexes reveals more significant and asymmetrical

conformational changes in the DNA binding lobe than in the dimerization region. Compared to apo-TcaR, binding of penicillin G resulted in a shortening of the distance between recognition helices (measured from Cα Lys65 to Cα Lys65′ of the other subunit) from 31.2 to 26.4 Å, whereas binding of other ligands induced different conformational changes, resulting in average displacements of recognition helices by 3.1–4.5 Å. Based on the distance of the recognition helices from each monomer, it was proposed that the unbound structure of TcaR is not pre-configured to bind DNA and the authors report that structural rearrangements would be required; such structural rearrangements might be restricted after associating with salicylate/antibiotics, resulting in attenuated DNA binding.

A shared ligand-binding pocket between dimerization and DNA-binding regions

The UrtR subset of MarR proteins includes several proteins that bind urate (Wilkinson and Grove 2004, Grove 2010, Perera and Grove 2010b, 2011, Huang *et al.* 2013, Wang *et al.* 2015, Deochand *et al.* 2016a). All proteins belonging to this family have four conserved amino residues, which are responsible for either coordinating ligand or for contributing to stability of the proteins. Genes encoding most of these homologs are divergently oriented to genes encoding membrane transport proteins that belong to either the drug metabolite transporter or the major facilitator superfamily, a notable exception being the founding member HucR from *D. radiodurans* that regulates the expression of a gene encoding uricase (Wilkinson and Grove 2004, 2005, Perera *et al.* 2009). Other urate-responsive proteins are PecS from the plant pathogens *Agrobacterium tumefaciens* (now designated as *A. fabrum*) (Perera and Grove 2010b) and *Pectobacterium atrosepticum* (Deochand *et al.* 2016a), the soil bacterium *S. coelicolor* (Huang *et al.* 2013), the human pathogen *Klebsiella pneumoniae* (Wang *et al.* 2015), and MftR from *Burkholderia thailandensis* (Gupta and Grove 2014).

HucR is very specific to urate. In contrast, *A. fabrum* and *S. coelicolor* PecS and *B. thailandensis* MftR bind both urate and xanthine and all are inferred to regulate gene expression in response to the production of purine catabolites that is induced in host cells upon infection, rationalizing why the ligand specificity differs from that of HucR. Notably, *S. coelicolor* TamR, which also belongs to the UrtR family, does not respond to urate or xanthine, but instead to citrate and related compounds associated with the citric acid cycle and it regulates the *tam* gene (encoding *trans*-aconitate methyltransferase) and other genes associated with the citric acid cycle in response to oxidative stress (Huang and Grove 2013, Huang *et al.* 2015). This difference in ligand specificity was ascribed to residues in α2, which line the predicted ligand-binding pocket, residues that are conserved among TamR proteins, but not in PecS and HucR (Huang and Grove 2013).

The predicted ligand binding sites of all UrtR homologs are based on the proposed model for interaction between HucR and urate and it was confirmed by mutagenesis of *A. fabrum* PecS. Urate binds in a crevice between the dimerization region and the DNA binding lobes at two symmetrical sites per HucR monomer with negative cooperativity. The occupancy of urate in the binding pocket results in displacement of recognition helices leading to attenuated DNA binding (Wilkinson and Grove 2005, Perera *et al.* 2009, Perera and Grove 2010b). The position of the ligand-binding pocket was also confirmed by mutagenesis of MftR (Gupta and Grove 2014), although different residues were inferred to contact ligand. Notably, the identified site matches the MTH313 main site (SAL1) and the ligand-binding site in *E. coli* MarR deduced by Duval et al. (Saridakis *et al.* 2008, Duval *et al.* 2013). It has also been reported that urate binding is communicated through the dimerization interface and that binding of urate at a single site destabilizes HucR, suggesting that ligand binding to a single site may suffice for attenuation of DNA binding (Gupta and Grove 2014, Deochand *et al.* 2016b). Similarly, binding of a single ligand to *Neisseria meningitidis* NadR, which represses expression of the virulence factor NadA, was inferred to stabilize a protein conformation that is incompatible with DNA binding (Liguori *et al.* 2016).

Catabolism of aromatic compounds

Comprehensive studies of MarR proteins that control expression of genes encoding enzymes involved in catabolism of aromatic compounds have yielded new insight into mechanisms by which ligand-binding may attenuate DNA binding. *S. coelicolor* PcaV is a transcription factor that regulates genes encoding enzymes involved in the β-ketoadipate pathway of protocatechuate (PCA) and catechol catabolism (Davis *et al.* 2013). Using Gibbs motif sampler, PcaV was predicted to bind two distinct 20 bp sites in the *pcaV–pcaI* intergenic region. Repression of gene activity by PcaV is attenuated by the anionic phenolic ligand PCA, and the structure of PcaV in complex with ligand reveals that two molecules of PCA bind PcaV in symmetrical binding pockets abutting the dimer interface. A comparison of apo and ligand bound-PcaV by superposition of the dimerization region shows that binding of ligand causes

the wHTH domains to rotate 15° upward towards the dimer interface (Figure 5). The altered conformation of PcaV is stabilized by Arg15, which interacts with bound PCA, in addition to residues from the wHTH domain. Further, this conformation is supported by residues from the *N*-terminal helix (α5), which becomes ordered upon PCA binding. Notably, mutational analysis of PcaV Arg15 illustrates that Arg15 plays a potential role in contacting both ligand and DNA.

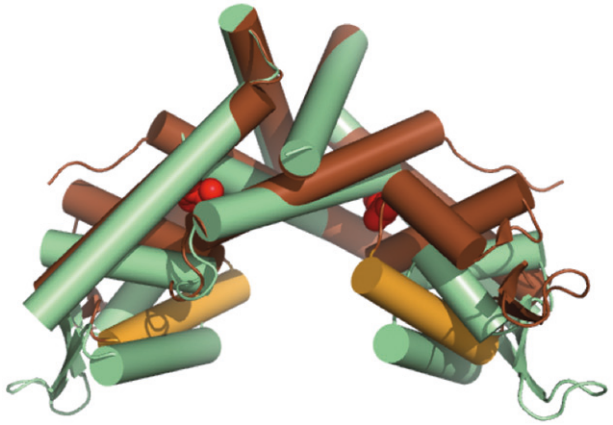

Figure 5. Ligand binding induces rigid-body movement of wHTH motif in PcaV. *S. coelicolor* PcaV (PDB ID: 4G9Y) shown in light green. Binding of ligand (protocatechuate; red) induces conformational changes in PcaV (PDB ID: 4FHT; brown) that include a rotation of recognition helices (gold). Superposition of structures is based on the dimerization region. Figure generated with PyMol. (see color version of this figure at www.tandfonline.com/ibmg).

In contrast, *Rhodococcus jostii* CouR is modulated by a unique mechanism (Otani *et al.* 2016). CouR represses the *cou* gene cluster, encoding enzymes required for *p*-hydroxycinnamate catabolism in this soil bacterium. Repression is lost in the presence of *p*-hydroxycinnamate-CoA, an intermediate of the pathway. The crystal structure of ligand-free CouR and its *p*-coumaroyl-CoA-bound form showed that two molecules of *p*-coumaroyl-CoA interact with a single CouR dimer. The *p*-coumaroyl-CoA ligands are bound in the cavity formed by two protomers of CouR, at the bottom of the dimerization region. The phenolic moieties of each ligand are inserted deep in hydrophobic binding pockets within each monomer, pockets that are remarkably similar to binding pockets in PcaV and UrtR homologs (Figure 6(B); magenta ligands). Intriguingly, the two CoA moieties adopt different configurations: one of the ligands interacts in an "extended" conformation along the helix α1 whereas the other binds in a "bent" conformation. By superimposing ligand-bound and apo-CouR, it was found that binding of *p*-coumaroyl-CoA failed to impose any conformational changes in the CouR structure. It was therefore suggested that both DNA and ligand compete for the same binding surface; indeed, phosphate moieties of the ligand interact with Arg36 and Arg38 of the wHTH motif. Thus, although binding of ligand does not cause structural changes, it alters the overall charge of the DNA binding surface and it sterically occludes key DNA binding residues.

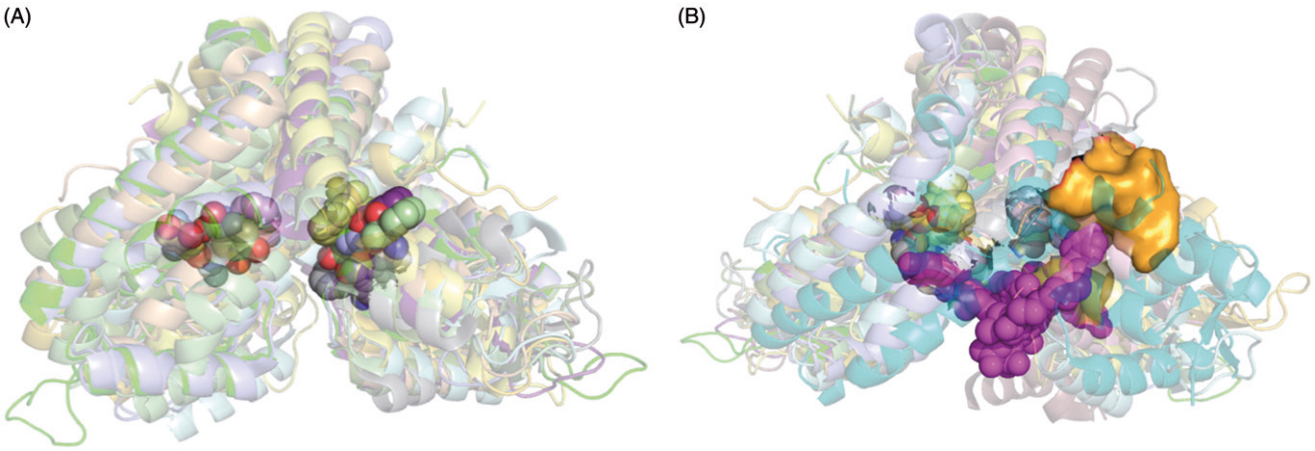

Figure 6. Superposition of MarR-ligand structures highlights conserved binding pocket. (A) Superposition of the following MarR-ligand structures with the proteins shown in semi-transparent cartoon and ligands in space-filling representation: MTH313-salicylate (3BPX), TcaR-salicylate (3KP6), Rv2887-salicylate (5HSN), SlyA-salicylate (3DEU), SAR2349-salicylate (4EM2), Absc-salicylate (3ZMD), ST1710-salicylate (3GF2), MepR-EtBr (5FFZ), HcaR-protocatechuate (4RGX), PcaV-protocatechuate (4FHT), NadR-4-hydroxyphenylacetate (5AIP). Several structures containing salicylate included multiple ligands, often surface-exposed, and only salicylate bound in the conserved pocket is shown. For some structures, only one ligand-binding pocket was occupied. (B) The same superposition as shown in (A) viewed from the opposite face and including MexR–ArmR (3ECH; ArmR in gold space-filling representation) and CouR-p-coumaroyl-CoA (5CYV; ligands in magenta; the p-coumaroyl moieties occupy the shared binding pockets, with CoA extending out). (see color version of this figure at www.tandfonline.com/ibmg).

Taken together, the structural analysis of available MarR proteins in complex with ligands combined with mutagenesis of predicted ligand-binding residues suggests that the ligand-binding pocket that is situated in a cleft between the dimerization and DNA-binding regions is shared among many MarR proteins (Figure 6(A)). Even bulky ligands such as the *p*-coumaroyl-CoA ligands for CouR bind with the phenolic moiety in the shared ligand binding pocket and CoA extending down (Figure 6(B); magenta ligands). However, while the pocket is conserved, the outcome of ligand binding may differ and range from conformational changes that lead to altered positions of recognition helices to placement of an extended ligand (CoA) across DNA-binding residues.

Conformational selection by ligand

A unique regulatory mechanism was reported for MexR, which negatively regulates the multidrug efflux pump MexAB-OprM in *P. aeruginosa* (Wilke *et al.* 2008). The expression of *mexAB-oprM* is additionally repressed by the TetR family proteins NalD and NalC, which also control production of the peptide ArmR. ArmR has been identified as an antirepressor of MexR and it prevents the binding of MexR to its target DNA *via* an allosteric protein–protein interaction. The crystal structure of ArmR-bound MexR shows that ArmR also binds MexR at the juncture of DNA binding and dimerization domains. The *C*-terminus of ArmR forms a kinked α-helix, which occupies the cavity, located at the bottom of the dimer interface, thus traversing the shared ligand-binding pocket (Figure 6(B); ArmR in gold). The binding of ArmR induces conformational changes that allosterically displace the MexR DNA binding lobes and generate an orientation that is incompatible with DNA binding (Figure 7).

It has also been suggested that DNA does not induce a conformational change in MexR. Instead, MexR was inferred to exist as an ensemble of conformations of which one is capable of DNA binding; mutation of Arg21 in helix α1 of the dimerization region to Trp prevents population of the state that is competent for DNA binding, emphasizing that dynamics of the dimer interface is integral to DNA binding. Since Arg21Trp mimics the phenotype of a ligand-bound derepressed state, the authors suggest that ligand-binding may likewise "freeze" the population in a state that is incompatible with DNA binding (Anandapadamanaban *et al.* 2016). This phenomenon was also inferred for NadR, where ligand (4-hydroxyphenylacetate) may selectively bind a subpopulation of NadR and lock it in conformation unsuitable for DNA binding (Liguori *et al.* 2016) and for

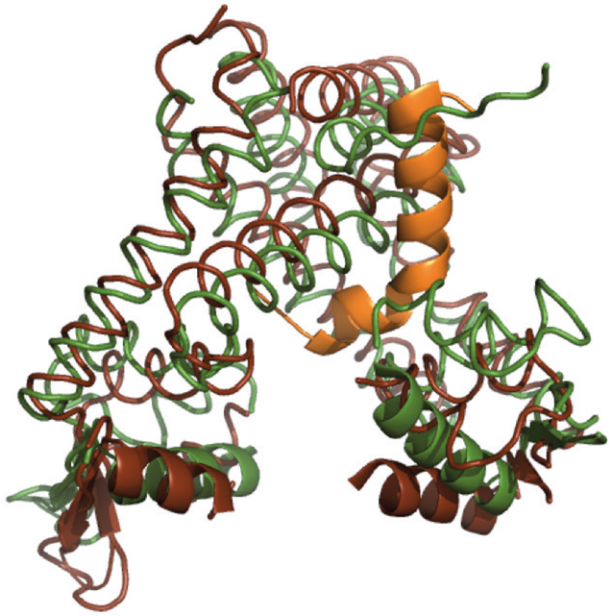

Figure 7. The binding of ArmR (gold cartoon) displaces the MexR DNA binding lobes to generate an orientation that is incompatible with DNA binding. Apo-MexR is in green (PDB ID: 1LNW) and MexR–ArmR in brown (PDB ID: 3ECH). Recognition helices are represented by cartoon. Figure generated with PyMol. (see color version of this figure at www.tandfonline.com/ibmg).

Acinetobacter baylyi ADP1 HcaR, for which ligand does not impose structural changes compared to apo-HcaR (Kim *et al.* 2016). Thus, a conformational selection may take place in which ligand shifts the conformational ensemble towards a conformation that is incompatible with DNA binding.

Regulation by metal binding

A MarR transcriptional regulator has been identified in *Streptococcus pneumoniae*, adhesin competence regulator (AdcR), which specifically modulates the expression of the Zn(II)-selective ABC transporter genes (*adcABC*) and a group of zinc binding proteins in presence of metals (Guerra *et al.* 2011). The co-crystallization of AdcR with Zn(II) identified two distinct metal-binding sites. Zn(II) at Site 1 is coordinated by residues His108, His112, His42, and Glu24 of helices α2 and α5 of the dimerization and DNA binding domains, while the Site 2 Zn(II) ion is coordinated by side chains of three residues (Cys30, Glu41, and Glu107) and by a water molecule (Figure 8). Mutational analysis indicates that only Site 1 is functionally relevant in the metalloregulatory mechanism of AdcR; notably, this site corresponds to the shared ligand-binding site for nonmetal ligands discussed above. The binding of zinc ion to the metal binding pocket induces a structural rearrangement that

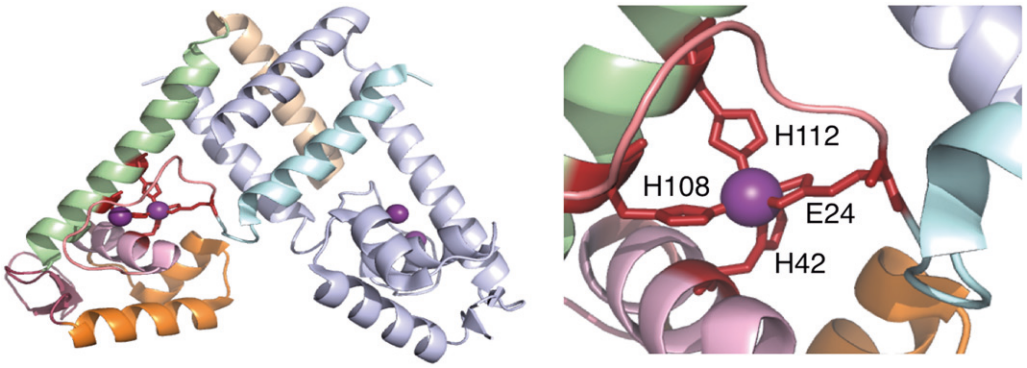

Figure 8. Zn^{2+} binding induces a conformation of AdcR that is compatible with DNA binding. Zn coordinating residues are shown in sticks (His108, His112, His42, and Glu24). Based on PDB ID: 3TGN. Figure generated with PyMol. (see color version of this figure at www.tandfonline.com/ibmg).

stabilizes the conformation of AdcR that is compatible with DNA binding.

The activity of *Lactobacillus brevis* TstR is also modulated in presence of metal (Pagliai *et al.* 2014). TstR represses the expression of the gene encoding the enzyme TstT by binding to the *tstRT* operon. TstT was identified as thiosulfate:cyanide sulfurtransferase that is involved in detoxification of cyanide. The DNA binding of TstR was altered by two molecules, sulfite and Fe(III), with sulfite promoting TstR binding to DNA and Fe(III) disrupting the protein–DNA complex resulting in expression of TstT. Intriguingly, Fe(III) promotes a protein–protein interaction between TstR and TstT, which was implicated in enhanced sulfurtransferase activity and an increased tolerance to cyanide. *In silico* analysis of a model structure of TstR predicted three ligand-binding sites, one located near the dimerization region with the other two in close proximity. Biochemical analysis and site-directed mutagenesis revealed that Site 1 serves as the binding site for sulfite while the other sites bind iron. Comparison of the structure of AdcR and the model of TstR revealed that predicted Site 1 is located at similar position as one of the binding sites for zinc in AdcR.

Sensors of oxidative stress

Living in an aerobic environment comes with a risk of being exposed to reactive oxygen species, which are generated as a by-product of cellular metabolism or when host cells mount a defense against stress or infection. Such species are derived from the sequential one-electron reduction of molecular oxygen or by Fenton's reaction, which is catalyzed by transition metals. An excess of reactive oxygen species can damage cellular components, including proteins, nucleic acids, and lipids (Keyer and Imlay 1996, Balasubramanian *et al.* 1998), and they can act as signaling molecules to induce antibiotic resistance phenotypes of pathogenic bacteria (Toledano *et al.* 2004, Antelmann and Helmann 2011). Upon sensing oxidative stress, bacterial cells induce expression of numerous genes that encode enzymes or compounds involved in detoxification of reactive oxygen species and in repair systems. Several proteins belonging to the MarR family have been implicated in controlling global virulence or antioxidant genes in response to oxidative stress (Liu *et al.* 2013).

Receptors for organic hydroperoxides

OhrR is an oxidative stress-sensing transcription factor that controls expression of *ohrA*, which encodes a peroxidase that catalyzes the reduction of organic hydroperoxides to the less toxic alcohols (Fuangthong and Helmann 2002, Hong *et al.* 2005, Newberry *et al.* 2007). The oxidation-sensing mechanism is mediated by one or more redox-active cysteine residues, which are involved in the formation of disulfide bonds or sulfenic acid derivatives. For instance, *B. subtilis* OhrR (BsOhrR) harbors a single cysteine (Cys15) at the *N*-terminus of helix α1; Cys15 is oxidized to form sulfenic acid in presence of organic hydroperoxide (Fuangthong and Helmann 2002). Although it was initially suggested that modification of the cysteine residues imposes conformational changes in BsOhrR that result in DNA binding attenuation, subsequent studies revealed that though sulfenylation is required, it is not sufficient to induce derepression and that formation of a cyclic sulfenamide or mixed disulfide formation with an intracellular thiol is required.

In contrast, *X. campestris* OhrR (XcOhrR) contains two redox active cysteines, Cys22 and Cys127, which are located on helix α1 and helix α5, respectively, and these residues are involved in formation of a disulfide bond (Newberry *et al.* 2007). Both OhrR proteins specifically

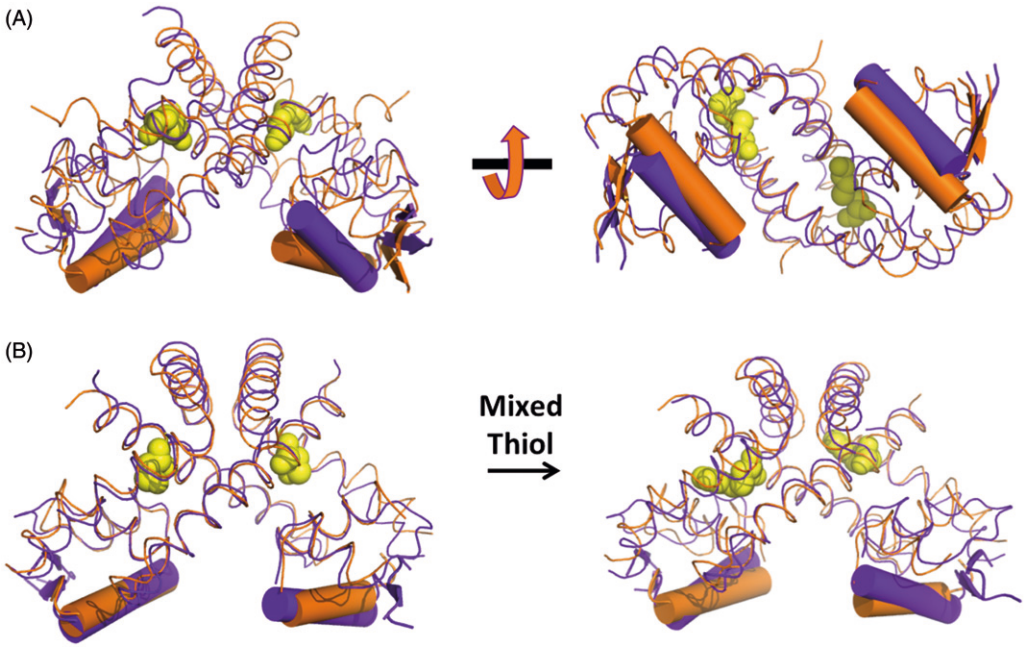

Figure 9. Conformational changes induced on protein oxidation. (A) Disulfide bond formation between C22 and C127′ (yellow spheres) upon oxidation of *X. campestris* OhrR causes structural rearrangements that are incompatible with DNA binding. Reduced (PDB ID: 2PEX; orange) and oxidized OhrR (PDB ID: 2PFB; purple) represented in ribbon form except for DNA recognition helices and wings (cartoon). (B) Structure of reduced (PDB ID: 3HSE; orange) SarZ is not altered significantly upon oxidation of Cys13 (yellow spheres) to sulfenic acid (PDB ID: 3HRM; purple; left panel). Further oxidation to generate a mixed disulfide (yellow spheres; PDB ID: 3HSR; purple) displaces DNA recognition helices compared to reduced SarZ (right panel). SarZ represented as ribbon except recognition helices and wings (cartoon). Figure generated with PyMol. (see color version of this figure at www.tandfonline.com/ibmg).

respond to only organic hydroperoxide, but not to hydrogen peroxide. Cysteine residues in XcOhrR are 15.5 Å apart, indicating that a large structural rearrangement would be necessary for the formation of the disulfide bond between these residues. A third cysteine residue, Cys131, does not appear to participate in oxidation sensing *in vivo*. Oxidation of XcOhrR by organic hydroperoxides results in disruption of helix α5, which allows Cys127 to perform a rotation of 135° and a translation of 8.2 Å towards Cys22 of *N*-terminal helix α1. Together, this maneuvering brings cysteine residues in close proximity and permits disulfide formation and it also induces swapping of helix α6 with α6′ of the other subunit without a significant alteration to the dimer interface. Further, it causes extension of helix α1 by one turn at the *N*- and *C*-termini leading to a 28° rotation of each wHTH domain and the attendant attenuation of DNA binding (Figure 9(A)).

Other redox sensors

Similar to BsOhrR, the lone cysteine in the *N*-terminal helix α1 in the dimerization region has been implicated in the redox sensing mechanism of global virulence regulators MgrA and SarZ from *S. aureus* (Chen *et al.* 2006, Poor *et al.* 2009). The sulfenylation of cysteine residues by oxidizing agent results in an allosteric change in the protein conformation and disruption of DNA binding. Intriguingly, MgrA is subject to other post-translational modifications such as serine or cysteine phosphorylation that can broaden the regulatory repertoire of this protein (Sun *et al.* 2012). The crystal structure of oxidized SarZ shows that the sulfenic acid form of Cys13 is stabilized by hydrogen bonding with neighboring residues and that the overall DNA binding conformation of the protein is retained (Figure 9(B)). However, further modification of Cys13-sulfenic acid with various thiols results in formation of a mixed disulfide, which displaces the recognition helix by 7 Å, a movement that would trigger steric clashes with DNA. In the examples described above, a redox-active cysteine from α1 is involved, rationalizing how conformational changes may propagate to the wHTH motifs; these conformational changes are nucleated at a position in proximity to the ligand-binding pocket shared among many MarR protein (Figure 6).

The majority of redox-responsive MarR proteins that have been characterized belong to a multiple cysteine subfamily. This includes MexR from *P. aeruginosa* that senses oxidative stress by formation of an interprotomer disulfide between redox-active cysteines (Cys30

and Cys62′) (Chen *et al.* 2008, 2010). Analysis of the oxidized MexR structure shows that interprotomer disulfide bond formation does not impact the dimerization domain or the distance between DNA recognition helices, however, it imposed conformational changes in the HTH domain, which precluded oxidized MexR from binding DNA. Thus, the repressor is released from the promoter region, allowing the expression of the *mexAB-oprM* regulon to mediate an antibiotic resistance phenotype.

Hypochloric acid-specific regulator (HypR) from *B. subtilis* and *Mycobacterium tuberculosis* MosR also employ a two-cysteine oxidation sensing mechanism (Brugarolas *et al.* 2012, Palm *et al.* 2012). However, unlike the redox-sensitive MarR proteins discussed above, HypR positively regulates the expression of flavin oxidoreductase HypO when it senses diamide stress due to NaOCl. The disulfide formation between Cys14–Cys49′ of HypR causes a reorientation of each subunit that moves the DNA recognition helices towards each other by 4 Å. This conformational change enables HypR to activate transcription of the *hypO* gene by promoting the binding of RNA polymerase to the *hypO* promoter (Palm *et al.* 2012). MosR is a negatively auto-regulatory protein that controls the induction of putative oxidoreductase, Rv1050. It contains four cysteine residues per monomer and forms two-intraprotomer disulfide bonds, one between Cys10–Cys12 and the other between Cys96–Cys147. However, structural studies show that only Cys10–Cys12 disulfide bond formation is a key modification in response to oxidative stress. The disulfide formation imposes rearrangement of hydrogen bonds and consequently rotation of the DNA binding helices α4 by ∼25°, which prevents them from interacting with consecutive major grooves (Brugarolas *et al.* 2012).

B. subtilis YodB controls expression of azoreductase AzoR1, the nitroreductase YodC, and the redox-sensing regulator Spx in response to diamide and quinones. These compounds deplete the cellular pool of low-molecular weight thiols and cause a stress response (Chi *et al.* 2010). YodB is modified by both diamide and quinones to produce an inter-subunit disulfide bond or S-alkylation, respectively, modifications that induce dissimilar conformational changes (Lee *et al.* 2016). Unmodified YodB is nearly identical to HypR, and the sulfur atoms of Cys6/Cys101′ are separated by 8–9 Å. Upon quinone-mediated alkylation of Cys6/Cys6′, the recognition helices move ∼3 Å towards each other, whereas diamide-mediated disulfide bond formation between Cys6 and Cys101′ results in significant conformational changes that alter the dimer interface and increase the distance between recognition helices to ∼60 Å. Thus, YodB undergoes unique conformational changes in response to the different signals, resulting in distinct functional outcomes.

In addition to reactive oxygen species, transition metals have also been implicated in redox sensing by MarR homologs. A notable example is *E. coli* MarR, which is oxidized by Cu^{2+} that is released from membrane proteins due to envelope stress induced by antibiotics, as discussed above (Hao *et al.* 2014). The functional consequence of protein oxidation is frequently an attenuation of DNA binding that releases repression. By contrast, Cu^{2+}-mediated oxidation of biofilm regulator BifR from *B. thailandensis* leads to formation of a disulfide bond between two BifR dimers to generate a dimer-of-dimers. *In vitro*, both reduced and oxidized BifR binds as a dimer-of-dimers to adjacent palindromes with little difference in affinity. *In vivo*, however, oxidative conditions result in further repression of BifR target genes, suggesting that oxidized BifR is a "super-repressor" that competes more efficiently for binding of RNA polymerase and that BifR functions as a rheostat (or dimmer-switch) to fine-tune gene activity in response to cellular redox state (Gupta *et al.* 2017).

Alternate regulatory mechanisms

Rheostats

As outlined above, modulation of MarR proteins by ligand binding or Cys oxidation in many cases induces or stabilizes a conformation in which DNA binding is attenuated, resulting in derepression of cognate genes, or a conformation in which enhanced DNA binding is linked to activation of target genes. In these scenarios, the MarR proteins operate as on-off switches, with inducing signal controlling the switch. By contrast, a few proteins appear to operate as rheostats, for example, *B. thailandensis* BifR, which appears to be converted into a "super-repressor" upon oxidation (Gupta *et al.* 2017). Another MarR regulator that falls into the "super-repressor" category of rheostats is *S. pneumoniae* FabT, which represses genes encoding enzymes involved in fatty acid biosynthesis. Upon association with acyl carrier protein (ACP) linked to long-chain fatty acyl chains, DNA binding by FabT is enhanced, ensuring efficient repression of *fab* genes under conditions of fatty acid sufficiency (Jerga and Rock 2009).

Repressor or activator?

Whereas the general DNA binding mechanism is similar for all MarR homologs, the position of operator sites relative to promoter elements determines whether the transcription factor will activate or repress gene

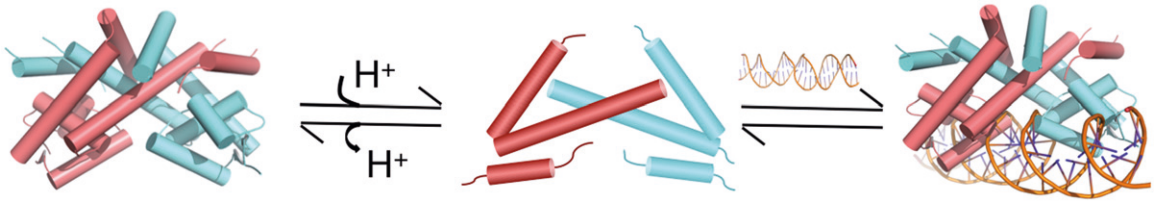

Figure 10. Protonation of stacked histidine residues at the pivot point of long helices that form the scaffold of the dimer interface of *D. radiodurans* HucR results in formation of reversible molten globule state (middle panel). A folded conformation of HucR is restored upon binding of cognate DNA. (see color version of this figure at www.tandfonline.com/ibmg).

expression. This is best illustrated by reduced *S. coelicolor* OhrR, which represses the expression of *ohrA* (encoding organic hydroperoxide reductase) and *ohrR* genes by promoter occlusion; however, oxidized OhrR loosely binds towards the −35 elements resulting in activation of the *ohrR* gene by interacting with alpha/sigma subunits of the RNA polymerase bound to the *ohrR* promoter without obstructing RNA polymerase binding to the *ohrA* promoter (Oh *et al.* 2007). Another example is RovA from *Y. pseudotuberculosis*, which activates transcription of the virulence gene *inv* by aiding the binding of RNA polymerase to the *inv* promoter (Tran *et al.* 2005).

Activation of gene activity may also be accomplished by competing for binding of a repressor. For example, the histone-like nucleoid-structuring protein H-NS is frequently associated with repression of gene expression, in particular expression of virulence genes, by bridging DNA to form repressive filaments (Grainger 2016). Expression of many genes that are activated by SlyA are subject to repression by H-NS, and activation has been suggested to be a consequence of SlyA antagonizing binding by H-NS (Colgan *et al.* 2016, Curran *et al.* 2017). Similarly, *Y. pseudotuberculosis* RovA, a homolog of SlyA, has been reported to antagonize H-NS-mediated gene silencing (Heroven *et al.* 2004, Tran *et al.* 2005).

In addition to regulating a single divergent gene or multiple genes in an operon, MarR transcription factors may also modulate the activity of distant genes by binding to the promoter region of these genes. For instance, PecS and MfbR from the phytopathogen *D. dadantii* have been shown to regulate several virulence genes or genes encoding cell wall degrading enzymes (*pelE*, *pelD*, *celZ*) (Reverchon *et al.* 1994, 2010). Thus they modulate a global gene network of the pathogens in response to the host defenses that are induced upon colonization. Similarly, MgrA or SarZ in *S. aureus* regulate a number of genes encoding virulence factors, efflux pumps, antibiotic resistance genes and other global regulatory genes involved in autolysis and metabolic pathways (Chen *et al.* 2006, 2009). Both transcription factors exert global regulation by triggering several defensive pathways in response to oxidative stress.

Molten globule formation

D. radiodurans HucR negatively controls expression of divergently oriented genes encoding HucR and uricase (Wilkinson and Grove 2004). In the presence of urate, the substrate for uricase, DNA binding is attenuated and the genes are expressed. However, HucR also responds to pH (Deochand *et al.* 2016b). The protonation of two stacked histidine residues (His51/His51′) at the pivot point of the long intersecting helices that nucleate the dimer interface (corresponding to α1 in Figure 2(A)) results in reversible formation of molten globule at pH 5.0 as evidenced in part by circular dichroism spectroscopy, which revealed a non-cooperative unfolding transition. Conversely, mutation of His51 to Phe restored the native protein fold at pH 5.0. While HucR failed to form stable protein–DNA complex at room temperature at pH 5.0, HucR was able to bind DNA at 4 °C, indicating that DNA partly restores the closely packed protein conformation. This suggests that HucR is sensitive to pH and contains a reversible molecular switch that can trigger the conversion of the folded state to a molten globule (Figure 10).

Hindering promoter escape

The *E. coli hpa-meta* operon encodes enzymes that catabolize 4-hydroxyphenylacetic acid (4HPA); it is repressed by HpaR and expression is induced by 4HPA (Prieto and Garcia 1997). DNase I footprinting revealed that HpaR binds two operator sites, OPR1 centered at +2 and OPR2 centered at −199 relative to the transcriptional start of *hpaG* (Galan *et al.* 2003). Both binding sites consist of two inverted half-sites of 9 bp separated by 4 bp. HpaR preferentially binds OPR1 to repress the *hpa-meta* operon when inducers are absent, followed by cooperative binding to OPR2, which leads to repression of *hpaR* expression. Notably, simultaneous binding of HpaR and RNA polymerase combined with an altered pattern of permanaganate footprinting suggests that

HpaR does not hinder the binding of RNA polymerase to the *hpa* promoter; rather it moves the RNA polymerase from its typical location, thereby preventing promoter escape. Moreover, the ternary complex formed by binding of RNA polymerase and HpaR to the promoter may restrict the formation of open complex at the transcriptional start site, further obstructing transcriptional initiation. In addition, OPR2 is centered at +47 relative to the start site of the *hpaR* gene, suggesting that HpaR binding to this site interferes with elongation. Considering the cooperative binding of HpaR to OPR1 and OPR2, it was proposed that two HpaR dimers bound to each of these sites might create a repression loop, perhaps stabilized by binding of the DNA-binding protein Integration Host Factor (IHF).

Altering promoter DNA topology

PecS from the soft-rot enterobacterium *P. atrosepticum* represses divergently oriented *pecS* and *pecM* genes in the conventional fashion by binding specifically to the *pecS–pecM* intergenic region (Deochand *et al.* 2016a). PecS is a member of the UrtR subfamily, and DNA binding is attenuated by urate; as a consequence, expression of *pecS* and *pecM* is increased.

However, DNA binding by *P. atrosepticum* PecS is also regulated by changes in pH. While the affinity of *P. atrosepticum* PecS only marginally decreases on raising the pH from 7 to 8 (an ~2-fold change in Kd), the mode of binding is different. DNase I footprinting revealed that PecS protects two palindromic regions (S1 and S2) in the *pecS–pecM* intergenic region and induces marked DNA distortion upon binding as evidenced by the presence of hypersensitive sites flanking each protected region; these hypersensitive cleavage sites are detected at neutral pH, the pH at which PecS represses gene activity *in vivo*. By contrast, DNA distortion is attenuated at a modestly alkaline pH, conditions under which *pecS* and *pecM* genes are expressed (Figure 11). Mutational analysis indicated that a specific histidine (His142) positioned at the junction of dimerization and DNA binding regions is key to pH-dependent regulation of gene activity by PecS. These observations led to the inference that DNA distortion imposed by binding of His142-protonated PecS hinders the binding RNA polymerase to the promoter region by altering the relative placement of −10 and −35 promoter elements; upon deprotonation of PecS, binding is no longer associated with a change in DNA topology, allowing RNA polymerase to compete for binding to the promoter and initiate transcription (Deochand *et al.* 2016a). Since the bacteria alkalinize the otherwise mildly acidic plant apoplast upon infection, the physiological relevance of pH-dependent regulation is the upregulation of virulence genes in the PecS regulon under these circumstances.

MarR proteins in biosensor devices

MarR family transcription factors excel at sensing and responding to chemical signals ranging from antibiotics

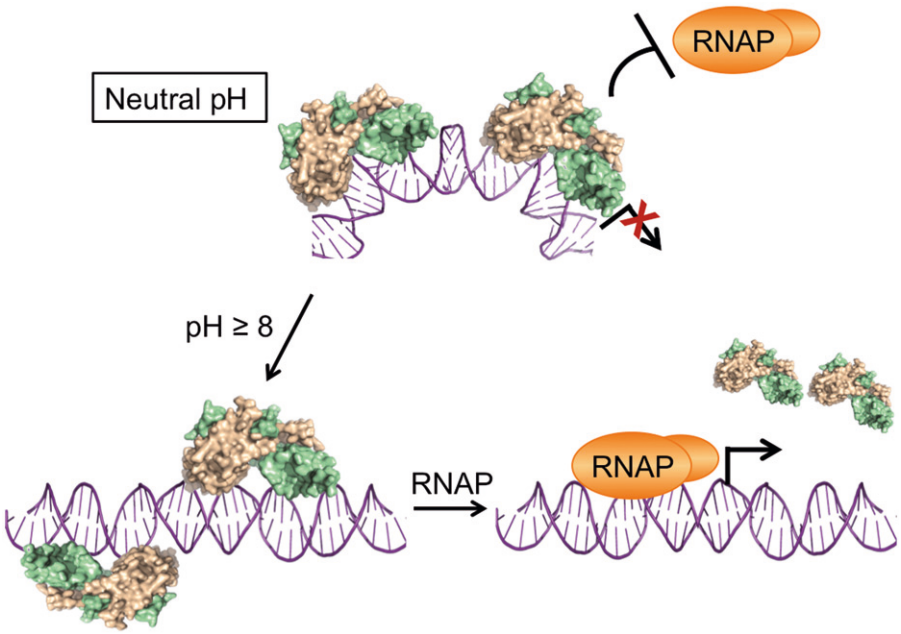

Figure 11. pH-dependent regulation of gene expression. *P. atrosepticum* PecS induces DNA distortion at neutral pH when binding to two sites in the *pecS–pecM* intergenic region, leading to repression of gene activity. At alkaline pH, DNA distortion is attenuated, allowing RNA polymerase (RNAP; orange) to compete for binding to the promoter region and initiate transcription. RNA polymerase not drawn to scale. (see color version of this figure at www.tandfonline.com/ibmg).

to metabolic intermediates and hydroxyl radicals. This property makes them excellent sensors in synthetic network circuits or devices that can detect pathological concentrations of specific metabolites and trigger corrective responses to ensure cellular homeostasis. One such synthetic circuit (urate-responsive expression network) was created using *D. radiodurans* HucR. Microencapsulated cells expressing a prosthetic gene network in which HucR senses elevated urate levels and mediates a dose-dependent derepression of a gene encoding *Apergillus flavus* urate oxidase were shown to reduce serum urate levels in mice (Kemmer *et al.* 2010). A separate device was created in which HucR bound to its cognate DNA crosslinks a hydrogel in which urate oxidase is trapped. On detecting the pathological urate concentration, HucR dissociates from DNA resulting in dissolution of the hydrogel and release of urate oxidase (Geraths *et al.* 2013). These devices can be used to target acute hyperuricemia, which is characterized by deposition of urate crystals in kidney, joints or other subcutaneous tissue and excess urate in blood that triggers inflammatory responses. Considering that HucR also responds to pH, it would be interesting to construct similar genetic network devices that may operate as pH sensors. This approach could be instrumental in targeting diseases that involves metabolic acidosis. These findings indicate that MarR proteins can be used in synthetic devices designed to curb certain metabolic or inflammatory disorders.

MarR-dependent genetic circuits designed for molecular recognition as opposed to an effect on host cell physiology have also been created. HucR again features as an example: Purified HucR and its cognate DNA were separately immobilized on donor and acceptor beads; addition of urate dissociates HucR from the DNA and causes separation between donor and acceptor beads and reduced emission of a luminescent signal (Li *et al.* 2016).

Whole cell-based biosensors have also been reported. For example, BldR from the thermophilic crenarchaeon *Sulfolobus solfataricus* activates expression of the gene encoding alcohol dehydrogenase (ADH) in presence of toxic aromatic aldehydes. This protein was expressed in *E. coli* in combination with a reporter in which the *ADH* gene promoter was fused to enhanced green fluorescent protein (eGFP). This biosensor strain exhibited a dose-dependent induction of eGFP in response to benzaldehyde (Fiorentino *et al.* 2009). *X. campestris* OhrR is oxidized by organic hydroperoxides to generate an inter-subunit disulfide bond, as discussed above (Newberry *et al.* 2007). Helix α5 is intact in reduced OhrR, and it is broken into two shorter helices connected by a loop upon oxidation. Insertion of a conformationally sensitive fluorescent reporter into this loop-region resulted in a sensor that exhibits enhanced fluorescence emission in presence of organic hydroperoxides (Zhao *et al.* 2010). While metabolic engineering to change metabolic fluxes remains challenging due to adverse effects on linked networks, the use of MarR proteins in sensor devices have clearly met with notable successes.

Concluding remarks

MarR proteins serve critical roles in control of cellular metabolism and in responses to environmental cues. In this capacity, they frequently function to control virulence genes. While all MarR proteins share a common wHTH scaffold in which the homodimeric transcription factor binds adjacent DNA major grooves, structural analyses have highlighted the distinct mechanisms by which the proteins engage cognate DNA. Such differences may, for example, explain the sequence-specificity exhibited by many MarR proteins, yet rationalize the ability of others to bind degenerate sites.

E. coli MarR has long been considered a classical example of how ligand-binding results in attenuation of DNA binding based on *in vitro* demonstration that salicylate attenuates DNA binding and crystallographic identification of salicylate binding sites. However, this mode of regulation has recently been firmly refuted. The current model for how salicylate and antibiotics result in attenuated DNA binding instead posits that envelope stress induced by exposure to antibiotics results in release of redox-active metals such as Cu^{2+} from envelope proteins. Cu^{2+} in turn oxidizes MarR to induce a tetramerization that buries the DNA recognition helices.

Analyses of several MarR proteins suggest that a crevice located between the dimerization region and DNA-binding lobes constitutes a shared ligand-binding pocket; ligand-binding to this site may for example result in conformational changes that lead to attenuated DNA binding or to direct obstruction of DNA recognition helices, depending on the size of the ligand. Interestingly, mutagenesis and molecular dynamics simulations indicate that some MarR proteins may exist as an ensemble of structures and that ligand-binding to a subset of this ensemble may instead "freeze" the population in a state that is incompatible with DNA binding. The location of the binding pocket predicts that ligand binding is communicated across the dimer interface; this inference is supported by the observation that substitutions in the dimer interface significantly impact both DNA and ligand binding. In addition, regulation of MarR protein function by reversible formation of a

molten globule state at acidic pH due to protonation of residues in the dimer interface has been documented. A functional significance is that flexibility of the dimer interface is essential for specific DNA binding and for an optimal response to inducing signal. Evidently, functional consequences of ligand binding vary between MarR homologs and must be determined on an individual basis.

Disclosure statement

The authors report no conflicts of interest.

Funding

This work was supported by the National Science Foundation [MCB-1515349 to A.G.].

ORCID

Dinesh K. Deochand http://orcid.org/0000-0002-7395-9250
Anne Grove http://orcid.org/0000-0002-4390-0354

References

Alekshun, M.N., Kim, Y.S., and Levy, S.B., 2000. Mutational analysis of MarR, the negative regulator of *marRAB* expression in *Escherichia coli*, suggests the presence of two regions required for DNA binding. *Molecular microbiology*, 35, 1394–1404.

Alekshun, M.N. and Levy, S.B., 1999a. Characterization of MarR superrepressor mutants. *Journal of bacteriology*, 181, 3303–3306.

Alekshun, M.N. and Levy, S.B., 1999b. The mar regulon: multiple resistance to antibiotics and other toxic chemicals. *Trends in microbiology*, 7, 410–413.

Alekshun, M.N. and Levy, S.B., 2007. Molecular mechanisms of antibacterial multidrug resistance. *Cell*, 128, 1037–1050.

Alekshun, M.N., *et al*., 2001. The crystal structure of MarR, a regulator of multiple antibiotic resistance, at 2.3 A resolution. *Nature structural biology*, 8, 710–714.

Anandapadamanaban, M., *et al*., 2016. Mutation-induced population shift in the MexR conformational ensemble disengages DNA binding: a novel mechanism for MarR family derepression. *Structure*, 24, 1311–1321.

Andresen, C., *et al*., 2010. Critical biophysical properties in the *Pseudomonas aeruginosa* efflux gene regulator MexR are targeted by mutations conferring multidrug resistance. *Protein science*, 19, 680–692.

Antelmann, H. and Helmann, J.D., 2011. Thiol-based redox switches and gene regulation. *Antioxidants & redox signaling*, 14, 1049–1063.

Balasubramanian, B., Pogozelski, W.K., and Tullius, T.D., 1998. DNA strand breaking by the hydroxyl radical is governed by the accessible surface areas of the hydrogen atoms of the DNA backbone. *Proceedings of the national academy of sciences of the United States*, 95, 9738–9743.

Birukou, I., *et al*., 2014. Structural mechanism of transcription regulation of the *Staphylococcus aureus* multidrug efflux operon mepRA by the MarR family repressor MepR. *Nucleic acids research*, 42, 2774–2788.

Bordelon, T., *et al*., 2006. The crystal structure of the transcriptional regulator HucR from *Deinococcus radiodurans* reveals a repressor preconfigured for DNA binding. *Journal of molecular biology*, 360, 168–177.

Brugarolas, P., *et al*., 2012. The oxidation-sensing regulator (MosR) is a new redox-dependent transcription factor in *Mycobacterium tuberculosis*. *Journal of biological chemistry*, 287, 37703–37712.

Chang, Y.M., *et al*., 2014. TcaR–ssDNA complex crystal structure reveals new DNA binding mechanism of the MarR family proteins. *Nucleic acids research*, 42, 5314–5321.

Chang, Y.M., *et al*., 2010. Structural study of TcaR and its complexes with multiple antibiotics from *Staphylococcus epidermidis*. *Proceedings of the national academy of sciences of the United States of America*, 107, 8617–8622.

Chen, H., *et al*., 2008. The *Pseudomonas aeruginosa* multidrug efflux regulator MexR uses an oxidation-sensing mechanism. *Proceedings of the national academy of sciences of the United States of America*, 105, 13586–13591.

Chen, H., *et al*., 2010. Structural insight into the oxidation-sensing mechanism of the antibiotic resistance of regulator MexR. *EMBO reports*, 11, 685–690.

Chen, P.R., *et al*., 2006. An oxidation-sensing mechanism is used by the global regulator MgrA in *Staphylococcus aureus*. *Nature chemical biology*, 2, 591–595.

Chen, P.R., *et al*., 2009. A new oxidative sensing and regulation pathway mediated by the MgrA homologue SarZ in *Staphylococcus aureus*. *Molecular microbiology*, 71, 198–211.

Chi, B.K., *et al*., 2010. The paralogous MarR/DUF24-family repressors YodB and CatR control expression of the catechol dioxygenase CatE in *Bacillus subtilis*. *Journal of bacteriology*, 192, 4571–4581.

Colgan, A.M., *et al*., 2016. The impact of 18 ancestral and horizontally-acquired regulatory proteins upon the transcriptome and sRNA landscape of *Salmonella enterica* serovar typhimurium. *PLoS genetics*, 12, e1006258.

Curran, T.D., *et al*., 2017. Identification of new members of the *Escherichia coli* K-12 MG1655 SlyA regulon. *Microbiology*, 163, 400–409.

Davis, J.R., *et al*., 2013. Study of PcaV from *Streptomyces coelicolor* yields new insights into ligand-responsive MarR family transcription factors. *Nucleic acids research*, 41, 3888–3900.

Deochand, D.K., Meariman, J.K., and Grove, A., 2016a. pH-dependent DNA distortion and repression of gene expression by *Pectobacterium atrosepticum* PecS. *ACS chemical biology*, 11, 2049–2056.

Deochand, D.K., *et al*., 2016b. Histidine switch controlling pH-dependent protein folding and DNA binding in a transcription factor at the core of synthetic network devices. *Molecular biosystems*, 12, 2417–2426.

Dolan, K.T., Duguid, E.M., and He, C., 2011. Crystal structures of SlyA protein, a master virulence regulator of *Salmonella*, in free and DNA-bound states. *Journal of biological chemistry*, 286, 22178–22185.

Duval, V., *et al*., 2013. Mutational analysis of the multiple-antibiotic resistance regulator MarR reveals a ligand binding

pocket at the interface between the dimerization and DNA binding domains. *Journal of bacteriology*, 195, 3341–3351.

Fiorentino, G., Ronca, R., and Bartolucci, S., 2009. A novel *E. coli* biosensor for detecting aromatic aldehydes based on a responsive inducible archaeal promoter fused to the green fluorescent protein. *Applied microbiology and biotechnology*, 82, 67–77.

Fuangthong, M. and Helmann, J.D., 2002. The OhrR repressor senses organic hydroperoxides by reversible formation of a cysteine-sulfenic acid derivative. *Proceedings of the national academy of sciences of the United States*, 99, 6690–6695.

Galan, B., *et al*., 2003. Molecular determinants of the hpa regulatory system of *Escherichia coli*: the HpaR repressor. *Nucleic acids research*, 31, 6598–6609.

Geraths, C., *et al*., 2013. A biohybrid hydrogel for the urate-responsive release of urate oxidase. *Journal of controlled release*, 171, 57–62.

Grainger, D.C., 2016. Structure and function of bacterial H-NS protein. *Biochemical society transactions*, 44, 1561–1569.

Groisman, E.A. and Mouslim, C., 2006. Sensing by bacterial regulatory systems in host and non-host environments. *Nature Reviews Microbiology*, 4, 705–709.

Grove, A., 2010. Urate-responsive MarR homologs from *Burkholderia*. *Molecular biosystems*, 6, 2133–2142.

Grove, A., 2013. MarR family transcription factors. *Current biology*, 23, R142–R143.

Guerra, A.J., *et al*., 2011. Crystal structure of the zinc-dependent MarR family transcriptional regulator AdcR in the Zn(II)-bound state. *Journal of the American Chemical Society*, 133, 19614–19617.

Gupta, A., Fuentes, S.M., and Grove, A., 2017. Redox-sensitive MarR homologue BifR from *Burkholderia thailandensis* regulates biofilm formation. *Biochemistry*, 56, 2315–2327.

Gupta, A. and Grove, A., 2014. Ligand-binding pocket bridges DNA-binding and dimerization domains of the urate-responsive MarR homologue MftR from *Burkholderia thailandensis*. *Biochemistry*, 53, 4368–4380.

Haider, F., *et al*., 2008. DNA recognition by the *Salmonella enterica* serovar typhimurium transcription factor SlyA. *International microbiology*, 11, 245–250.

Hao, Z., *et al*., 2014. The multiple antibiotic resistance regulator MarR is a copper sensor in *Escherichia coli*. *Nature chemical biology*, 10, 21–28.

Heroven, A.K., *et al*., 2004. RovA is autoregulated and antagonizes H-NS-mediated silencing of invasin and rovA expression in *Yersinia pseudotuberculosis*. *Molecular microbiology*, 53, 871–888.

Hong, M., *et al*., 2005. Structure of an OhrR–ohrA operator complex reveals the DNA binding mechanism of the MarR family. *Molecular cell*, 20, 131–141.

Huang, H. and Grove, A., 2013. The transcriptional regulator TamR from *Streptomyces coelicolor* controls a key step in central metabolism during oxidative stress. *Molecular microbiology*, 87, 1151–1166.

Huang, H., Mackel, B.J., and Grove, A., 2013. *Streptomyces coelicolor* encodes a urate-responsive transcriptional regulator with homology to PecS from plant pathogens. *Journal of bacteriology*, 195, 4954–4965.

Huang, H., Sivapragasam, S., and Grove, A., 2015. The regulatory role of *Streptomyces coelicolor* TamR in central metabolism. *Biochemical journal*, 466, 347–358.

Jerga, A. and Rock, C.O., 2009. Acyl–Acyl carrier protein regulates transcription of fatty acid biosynthetic genes via the FabT repressor in *Streptococcus pneumoniae*. *Journal of biological chemistry*, 284, 15364–15368.

Kaatz, G.W., Demarco, C.E., and Seo, S.M., 2006. MepR, a repressor of the *Staphylococcus aureus* MATE family multidrug efflux pump MepA, is a substrate-responsive regulatory protein. *Antimicrobial agents and chemotherapy*, 50, 1276–1281.

Kemmer, C., *et al*., 2010. Self-sufficient control of urate homeostasis in mice by a synthetic circuit. *Nature biotechnology*, 28, 355–360.

Kersey, P.J., *et al*., 2016. Ensembl Genomes 2016: more genomes, more complexity. *Nucleic Acids Research*, 44, D574–D580.

Keyer, K. and Imlay, J.A., 1996. Superoxide accelerates DNA damage by elevating free-iron levels. *Proceedings of the national academy of sciences of the United States of America*, 93, 13635–13640.

Kim, Y., *et al*., 2016. How aromatic compounds block DNA binding of HcaR catabolite regulator. *Journal of biological chemistry*, 291, 13243–13256.

Kumaraswami, M., *et al*., 2009. Structural and biochemical characterization of MepR, a multidrug binding transcription regulator of the *Staphylococcus aureus* multidrug efflux pump MepA. *Nucleic acids research*, 37, 1211–1224.

Kumarevel, T., *et al*., 2009. ST1710-DNA complex crystal structure reveals the DNA binding mechanism of the MarR family of regulators. *Nucleic acids research*, 37, 4723–4735.

Lee, S.J., *et al*., 2016. Two distinct mechanisms of transcriptional regulation by the redox sensor YodB. *Proceedings of the national academy of sciences*, 113, E5202–E5211.

Li, S., *et al*., 2016. A platform for the development of novel biosensors by configuring allosteric transcription factor recognition with amplified luminescent proximity homogeneous assays. *Chemical communications*, 53, 99–102.

Liguori, A., *et al*., 2016. Molecular basis of ligand-dependent regulation of NadR, the transcriptional repressor of meningococcal virulence factor NadA. *PLoS pathogens*, 12, e1005557.

Lim, D., Poole, K., and Strynadka, N.C., 2002. Crystal structure of the MexR repressor of the *mexRAB-oprM* multidrug efflux operon of *Pseudomonas aeruginosa*. *Journal of biological chemistry*, 277, 29253–29259.

Liu, X., *et al*., 2013. Oxidation-sensing regulator AbfR regulates oxidative stress responses, bacterial aggregation, and biofilm formation in *Staphylococcus epidermidis*. *Journal of biological chemistry*, 288, 3739–3752.

Liu, Z., Walton, T.A., and Rees, D.C., 2010. A reported archaeal mechanosensitive channel is a structural homolog of MarR-like transcriptional regulators. *Protein science*, 19, 808–814.

Newberry, K.J., *et al*., 2007. Structural mechanism of organic hydroperoxide induction of the transcription regulator OhrR. *Molecular cell*, 28, 652–664.

Oh, S.Y., Shin, J.H., and Roe, J.H., 2007. Dual role of OhrR as a repressor and an activator in response to organic hydroperoxides in *Streptomyces coelicolor*. *Journal of bacteriology*, 189, 6284–6292.

Otani, H., *et al*., 2016. The activity of CouR, a MarR family transcriptional regulator, is modulated through a novel molecular mechanism. *Nucleic acids research*, 44, 595–607.

Pagliai, F.A., *et al*., 2014. A dual role of the transcriptional regulator TstR provides insights into cyanide detoxification in *Lactobacillus brevis*. *Molecular microbiology*, 92, 853–871.

Palm, G.J., *et al*., 2012. Structural insights into the redox-switch mechanism of the MarR/DUF24-type regulator HypR. *Nucleic acids research*, 40, 4178–4192.

Perera, I.C. and Grove, A., 2010a. Molecular mechanisms of ligand-mediated attenuation of DNA binding by MarR family transcriptional regulators. *Journal of molecular cell biology*, 2, 243–254.

Perera, I.C. and Grove, A., 2010b. Urate is a ligand for the transcriptional regulator PecS. *Journal of molecular biology*, 402, 539–551.

Perera, I.C. and Grove, A., 2011. MarR homologs with urate-binding signature. *Protein science*, 20, 621–629.

Perera, I.C., *et al*., 2009. Mechanism for attenuation of DNA binding by MarR family transcriptional regulators by small molecule ligands. *Journal of molecular biology*, 390, 1019–1029.

Perez-Rueda, E., Collado-Vides, J., and Segovia, L., 2004. Phylogenetic distribution of DNA-binding transcription factors in bacteria and archaea. *Computational biology and chemistry*, 28, 341–350.

Poor, C.B., *et al*., 2009. Crystal structures of the reduced, sulfenic acid, and mixed disulfide forms of SarZ, a redox active global regulator in *Staphylococcus aureus*. *Journal of biological chemistry*, 284, 23517–23524.

Praillet, T., *et al*., 1996. Purification and functional characterization of PecS, a regulator of virulence-factor synthesis in *Erwinia chrysanthemi*. *Molecular microbiology*, 20, 391–402.

Prieto, M.A. and Garcia, J.L., 1997. Identification of a novel positive regulator of the 4-hydroxyphenylacetate catabolic pathway of *Escherichia coli*. *Biochemical and biophysical research communications*, 232, 759–765.

Reverchon, S., Nasser, W., and Robert-Baudouy, J., 1994. *pecS*: a locus controlling pectinase, cellulase and blue pigment production in *Erwinia chrysanthemi*. *Molecular microbiology*, 11, 1127–1139.

Reverchon, S., *et al*., 2010. Systematic targeted mutagenesis of the MarR/SlyA family members of *Dickeya dadantii* 3937 reveals a role for MfbR in the modulation of virulence gene expression in response to acidic pH. *Molecular microbiology*, 78, 1018–1037.

Rouanet, C., *et al*., 1999. Regulation of pelD and pelE, encoding major alkaline pectate lyases in *Erwinia chrysanthemi:* involvement of the main transcriptional factors. *Journal of bacteriology*, 181, 5948–5957.

Saridakis, V., *et al*., 2008. Structural insight on the mechanism of regulation of the MarR family of proteins: high-resolution crystal structure of a transcriptional repressor from *Methanobacterium thermoautotrophicum*. *Journal of molecular biology*, 377, 655–667.

Sun, F., *et al*., 2012. Protein cysteine phosphorylation of SarA/MgrA family transcriptional regulators mediates bacterial virulence and antibiotic resistance. *Proceedings of the national academy of sciences of the United States*, 109, 15461–15466.

Toledano, M.B., *et al*., 2004. Microbial H2O2 sensors as archetypical redox signaling modules. *Trends in biochemical sciences*, 29, 351–357.

Tran, H.J., *et al*., 2005. Analysis of RovA, a transcriptional regulator of *Yersinia pseudotuberculosis* virulence that acts through antirepression and direct transcriptional activation. *Journal of biological chemistry*, 280, 42423–42432.

Wang, Z.C., *et al*., 2015. PecS regulates the urate-responsive expression of type 1 fimbriae in *Klebsiella pneumoniae* CG43. *Microbiology*, 161, 2395–2409.

Wilke, M.S., *et al*., 2008. The crystal structure of MexR from *Pseudomonas aeruginosa* in complex with its antirepressor ArmR. *Proceedings of the national academy of sciences of the United States of America*, 105, 14832–14837.

Wilkinson, S.P. and Grove, A., 2004. HucR, a novel uric acid-responsive member of the MarR family of transcriptional regulators from *Deinococcus radiodurans*. *Journal of biological chemistry*, 279, 51442–51450.

Wilkinson, S.P. and Grove, A., 2005. Negative cooperativity of uric acid binding to the transcriptional regulator HucR from *Deinococcus radiodurans*. *Journal of molecular biology*, 350, 617–630.

Zhao, B.S., *et al*., 2010. A highly selective fluorescent probe for visualization of organic hydroperoxides in living cells. *Journal of the American chemical society*, 132, 17065–17067.

Zhu, R., *et al*., 2017. Structural characterization of the DNA-binding mechanism underlying the copper(II)-sensing MarR transcriptional regulator. *Journal of biological inorganic chemistry*, 22, 685–693.